Research on the Digital Twin for Thermal Characteristics of Motorized Spindle

Jianying Xiao

School of Mechanical Engineering, University of Shanghai for Science and Technology, Shanghai 200093, China

Fan Kai-Guo (fkg11@163.com)

University of Shanghai for Science and Technology

Research Article

Keywords: Digital twin, Thermal characteristics, Precision simulation, Motorized spindle

Posted Date: August 5th, 2021

DOI: https://doi.org/10.21203/rs.3.rs-767803/v1

Version of Record: A version of this preprint was published at The International Journal of Advanced Manufacturing Technology on January 14th, 2022. See the published version at https://doi.org/10.1007/s00170-021-08508-y.

Research on the digital twin for thermal characteristics of motorized spindle

Jianying Xiao, Kaiguo Fan*

School of Mechanical Engineering, University of Shanghai for Science and Technology, Shanghai 200093, China
Corresponding author. E-mail address: fkg11@163.com

Abstract
With the increase of spindle speed, heat generation becomes the crucial problem of high-speed motorized spindle. In order to obtain the actual thermal behavior of a motorized spindle, a digital twin system for thermal characteristics is developed in this paper. The mechanism of digital twin for thermal characteristics is to simulate the thermal behavior of a machine tool through mapping and correcting the thermal boundary conditions using the data acquisition system and correction models. The proposed digital twin system includes three modules which are the digital twin software, the data acquisition system, and the physical model with embedding sensors. The digital twin software is developed based on the Qt with the C++ programming language and the secondary development of ANSYS. Correction models for thermal boundaries are proposed to correct the heat generation and thermal contact resistance using the temperatures measured by the data acquisition system at thermal key points. To verify the prediction accuracy of the digital twin system, an experiment is carried out on a motorized spindle. The experimental results show that the prediction accuracy of the digital twin system is greater than 95%. It is of great significance to improve the accuracy of thermal characteristics simulation and thermal optimization.

Keywords Digital twin · Thermal characteristics · Precision simulation · Motorized spindle

1. Introduction

Thermal behavior prediction is significant in thermal optimization of Computer Numerical Control (CNC) machine tools. The motorized spindle is not only the core but also a main heat source of CNC machine tools. More rigorous requirement on accurate analysis of thermal characteristics of motorized spindle is put forward due to the fast development of CNC machine tools in condition of ultra-high speed and ultra-high precision. The main factors that affect the accurate prediction of the temperature field and thermal deformation of the spindle come from two aspects, heat generation and thermal contact resistance, both of which are not constant during the working process of the spindle. Owing to the heat generation goes with it as spindle works which cause the thermal deformation, the thermal stress between the contact surfaces of the spindle's components is engendered, and the Thermal Contact Resistance (TCR) and the heat generated by internal heat sources also change with the change of contact pressure. In order to improve the prediction accuracy of thermal behavior, digital twin for thermal characteristics becomes the best choice that is helpful in simulating the temperature field distribution of spindle unit.

Digital twin refers to a virtual and real mapping by constructing the mapping relationship between digital virtual entity and physical entity. It maps the physical entity in the physical space to the digital space, and has functions such as data mapping, analysis and decision-making, and control execution. In recent years, many scholars have carried out fruitful research work on digital twin and have formed a mature theoretical system. In the theoretical aspects, the concept of digital twin was proposed by Professor Grieves [1] in 2003 firstly, and later the NASA applied the concept to the aircraft in the Apollo program. Dmitry Kostenko et al. [2] studied the application of device digital twins in static and dynamic diagnosis, and proposed a knowledge base-based diagnosis method. Tao F et al. [3-5] constructed a five-dimensional structural model and driving-based application standards for the digital twin, and proposed 14 application hypotheses driven by the digital twin, and analyzed in detail the product design, manufacturing and service methods based on digital twin technology, which was applied to the equipment fault prediction and health management research. Besides, abundant relevant scholars emerged in the field of manufacturing [6-12]. Zheng et al. [13] studied the digital twin model framework of welding equipment, and realized the real-time monitoring of welding equipment based on OPCUA and Socket data collection, information preprocessing, and real-time data mapping. Luo et al. [14] have done research on the modeling method of digital twin of CNC machine tools, and proposed a digital twin framework of CNC with 3 dimensions including data description model, mapping model, and intelligent model. Eric J. Tuegel et al. [15] studied the problem of aircraft structure life prediction based on digital twin, and proposed a digital twin model for aircraft to integrate the calculation of structural deflection and temperature, thereby analyzing local damage and materials state evolution. The above works show that, digital twin has a wide range of applications and research in the field of mechanical engineering, and has displayed good results, with great applicability and malleability.

Under the framework of digital twin, the Finite Element Method (FEM) was utilized to simulate the thermal behavior of machine tools' spindle. Numerical methods have better reliability and convenience than traditional experiment methods in different machine tool or multifold experimental environment and can solve complex nonlinear problems. Chen et al. [16] and Su et al. [17] calculated the necessary thermal loads of hydrostatic oil films with the empirical method, as well as the utilization of the finite element method

and finite volume method to simulate temperature and thermal error behaviors of hydrostatic spindle unit, respectively. Zhou et al. [18] analyzed the thermal behavior of a machine tool's spindle using the FEM and proposed a thermal error reduction strategy for optimizing the thermal conductivity of the materials by designing a heat conduction and insulation device to achieve the rapid heat conduction and accelerate the thermal balance of the spindle, thereby the thermal errors is greatly reduced. Determining the thermal boundary conditions accurately is the key of FEM, but the boundary conditions of a spindle are not constant leading to the inaccuracy of the finite element analysis. To solve this problem, Xu et al. [19] analyzed the influence of thermal contact resistance on the accuracy of the FEM, the results suggested that the boundary conditions were connected with the analysis accuracy of the FEM. Jian et al. [20] developed a FEM to analyze the temperature distribution of a spindle system under the conditions of different rotational speeds, temperature rises, and thermal deformations. Fan [21] studied the linear relationships between the thermal deformation and the temperature rise as well as the heat flux and the temperature rise by using FEM, and designed an application to realize the real-time monitoring of the deformation and the temperature field of a machine tool. Zhang et al. [22] used fractal theory and FEM to study the temperature field of a machining center's spindle. Liu et al. [23] proposed a real-time compensation method, by which it is helpful to control the thermal error of machine tool.

In order to obtain the accurate boundary conditions that is the key of the FEM, the main types of boundary conditions related is named as heat generation rates, thermal contact resistances, and convective heat transfer coefficients [24]. Huang et al. [25] proposed an inverse method using the ANSYS parametric design language and the conjugate gradient method to acquire the estimated time-varying heat generations of the spindle bearings considering multifold conditions. Chow et al. [26] explore ways of getting the optimal convective heat transfer coefficient, and the simulated temperatures curves fit well with the experiment by using the FE thermal simulation analysis of a ball screw system in conclusion.

On the basis of previous studies, and the emphasis that the temperature field of a spindle is correlative with TCRs of contact surfaces, the convection heat transfer coefficients (CHTCs), and the heat generation of spindle system, a digital twin system for thermal behavior is introduced in this paper, which uses the real-time temperature data and simulation results to correct the thermal contact resistance of the spindle's contact surface and the heat generated by the internal heat sources by embedding the temperature sensors in the spindle. And a digital twin software is developed using the C++ to achieve the purpose of accurately simulating the temperature field and thermal deformation of the spindle. the digital twin mechanism for thermal behavior is clarified in section 2. The design strategy of digital twin system is introduced in section 3. The correction principle of thermal boundaries is expounded in section 4. Finally, the effect of the proposed digital twin system for thermal behavior is verified through simulation and experiment in section 5. The results show that the prediction accuracy of the proposed digital twin system for thermal behavior is greater than 95%, it is of great significance to improve the accuracy of thermal analysis and thermal optimization of CNC machine tools.

2. Digital twin mechanism for thermal behavior

Digital twin is a simulation process which integrates the multi-disciplines, multi-physical quantities, multi-scales, and multi-probability through using the physical models, sensors, historical data etc. The purpose of digital twin is using the finite element simulation to map the life cycle of an actual equipment to the virtual space to obtain the attribute changes of the equipment in the physical space.

The mechanism of digital twin for thermal characteristics is to simulate the thermal behavior of a machine tool through mapping and correcting the thermal boundary conditions using the data acquisition system and correction models. As shown in Fig. 1, the temperature-rise and thermal deformation of thermal key points related to the thermal boundary conditions of an actual machine tool are measured through embedding the temperature sensors. The measured data are transmitted to the digital twin system through multi-channel data acquisition system. The thermal boundary conditions used in the numerical simulation are corrected using the thermal boundary correction models. The corrected thermal boundary conditions are applied to the finite element model of the motorized spindle through ANSYS Parametric Design Language (APDL), and the thermal characteristic analysis of the motorized spindle is realized by calling the finite element simulation software.

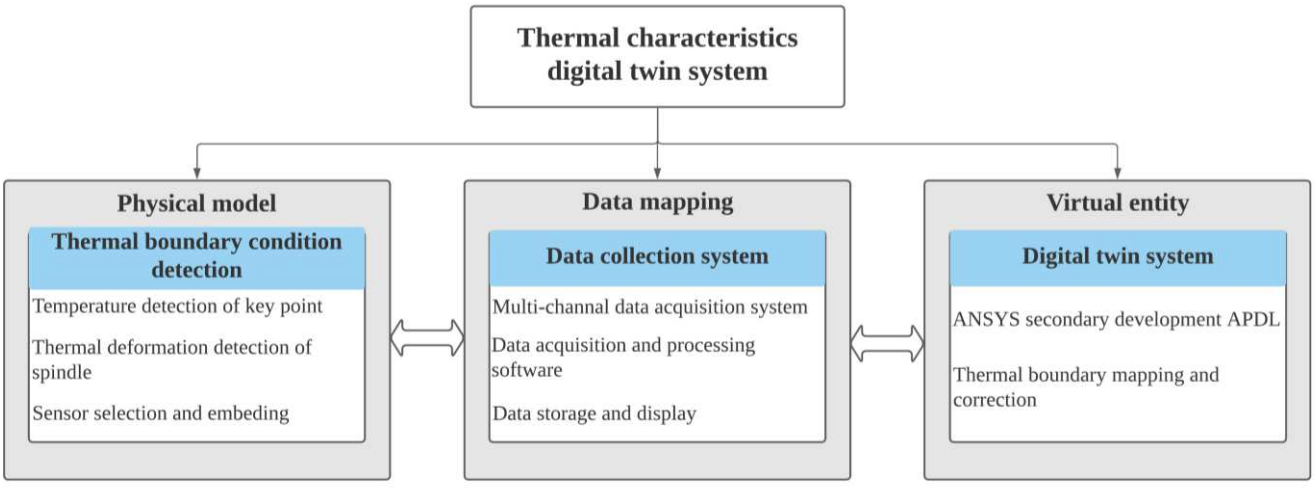

Fig.1 The digital twin mechanism for thermal characteristics

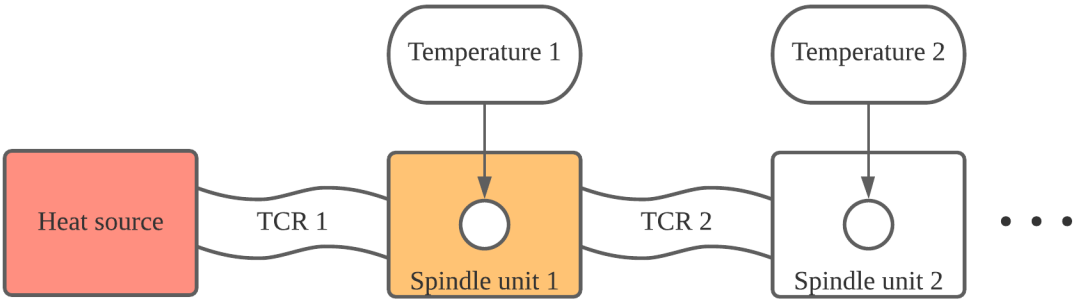

Fig.2 Correction mechanism of the thermal boundary conditions

The key of digital twin for thermal behavior is to map the thermal boundaries accurately using the embedded sensors and data acquisition system. However, it is difficult to install a sensor for each thermal boundary. Therefore, the online correction technique for thermal boundary conditions is proposed to correct the thermal boundaries real-timely. As shown in **Fig. 2**, the heat generated by the internal heat source is transferred to the spindle unit 1 through the Thermal Contact Resistance 1 (TCR1), and then to the spindle unit 2 through TCR2. The measured temperatures at position Temp.1 and 2 are transmitted to the digital twin system through the data collection system. The digital twin system calls APDL to calculate the temperature of each point. If the simulated temperatures at position Temp.1 and 2 are equal to the measured temperature at the same position, then the thermal boundaries used in the simulation is consistent with the actual thermal boundaries. If the simulated temperatures are not equal to the measured temperatures, the thermal boundary correction models are called to correct the thermal boundaries according to the difference between simulated and measured temperature. Finally, the accurate thermal boundary conditions can be identified. Using the corrected thermal boundaries, the actual thermal characteristics of the spindle can be obtained through digital twin simulation.

3. Design strategy of digital twin system

A digital twin system for thermal behavior includes three modules that are the digital twin software, the data acquisition system, and the physical model with embedding sensors. The design strategy of digital twin system for thermal behavior is to design these three modules according to the digital twin mechanism for thermal behavior.

3.1 Design of digital twin software

The digital twin software is developed using the Qt software based on the C++ programming language. The main functions of the digital twin software include the setting of initial boundary conditions, establishing the connection with the Internet of Things based Data Acquisition System (IoT-DAS), calling the ANSYS software, displaying data information and solution results, and saving the simulated data.

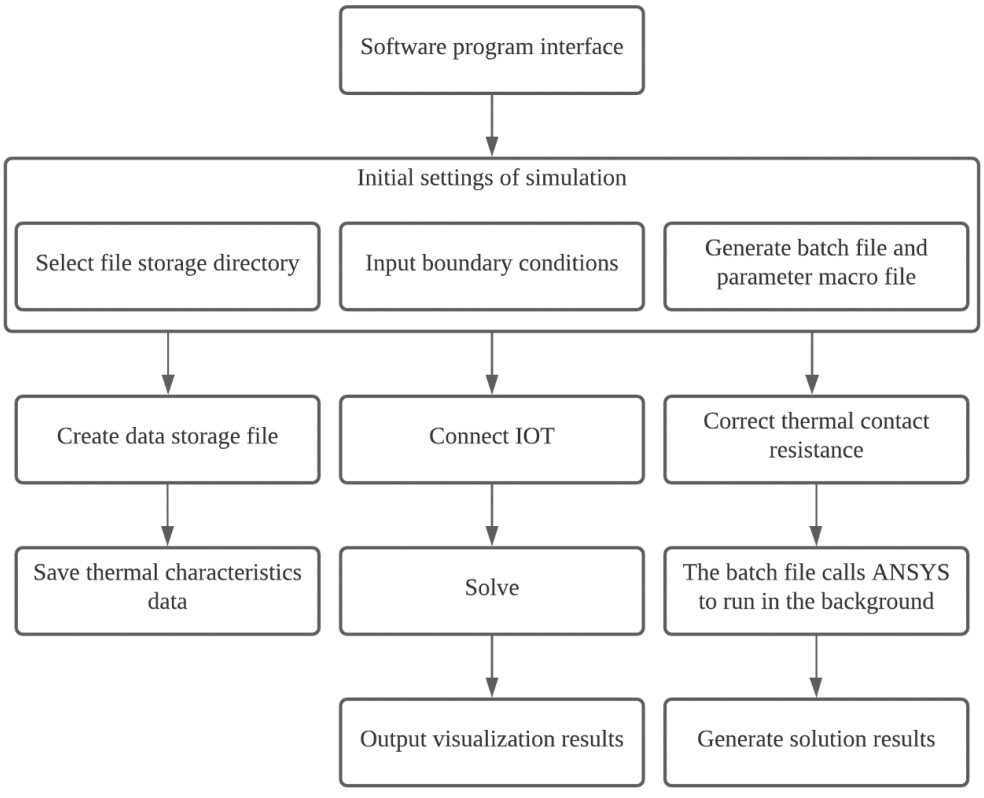

Fig.3 The flow chart of digital twin software for thermal characteristics

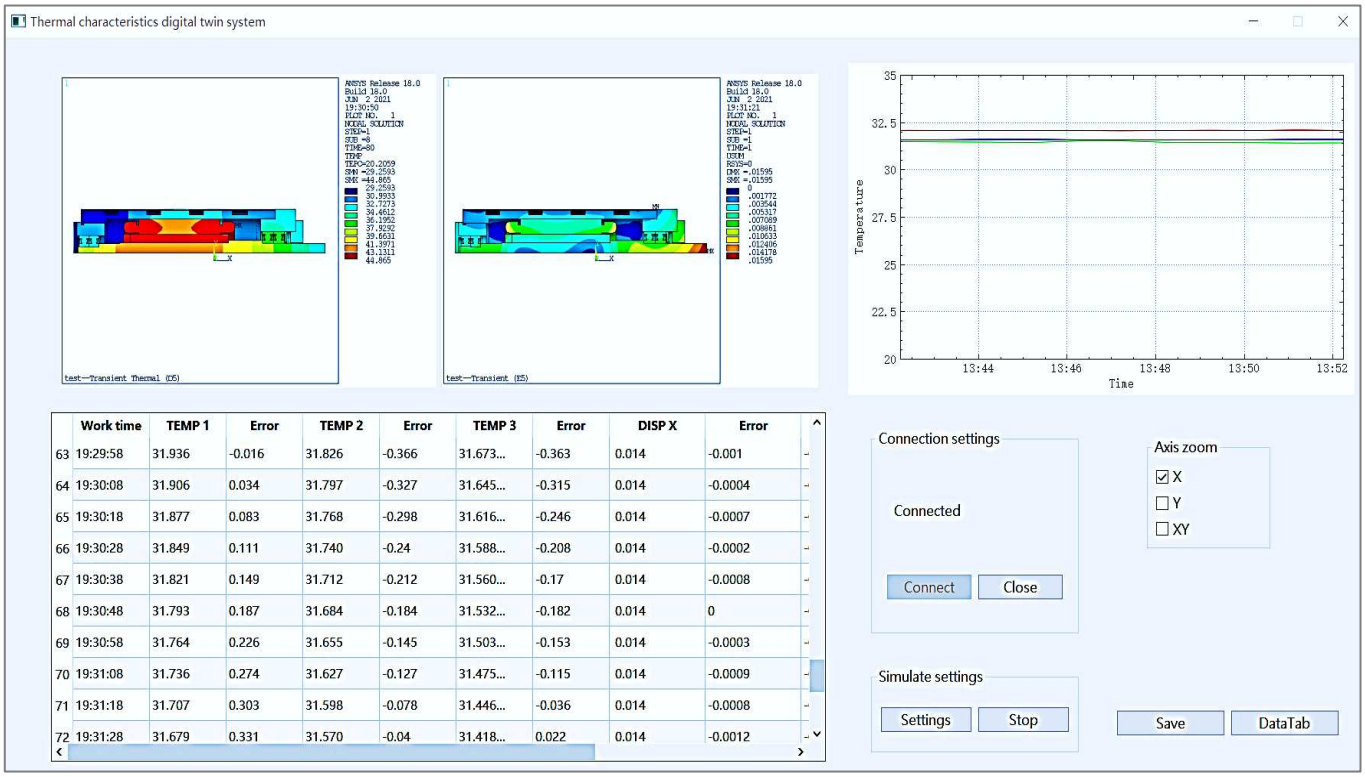

	Work time	TEMP 1	Error	TEMP 2	Error	TEMP 3	Error	DISP X	Error
63	19:29:58	31.936	-0.016	31.826	-0.366	31.673...	-0.363	0.014	-0.001
64	19:30:08	31.906	0.034	31.797	-0.327	31.645...	-0.315	0.014	-0.0004
65	19:30:18	31.877	0.083	31.768	-0.298	31.616...	-0.246	0.014	-0.0007
66	19:30:28	31.849	0.111	31.740	-0.24	31.588...	-0.208	0.014	-0.0002
67	19:30:38	31.821	0.149	31.712	-0.212	31.560...	-0.17	0.014	-0.0008
68	19:30:48	31.793	0.187	31.684	-0.184	31.532...	-0.182	0.014	0
69	19:30:58	31.764	0.226	31.655	-0.145	31.503...	-0.153	0.014	-0.0003
70	19:31:08	31.736	0.274	31.627	-0.127	31.475...	-0.115	0.014	-0.0009
71	19:31:18	31.707	0.303	31.598	-0.078	31.446...	-0.036	0.014	-0.0008
72	19:31:28	31.679	0.331	31.570	-0.04	31.418...	0.022	0.014	-0.0012

Fig.4 The interface of digital twin system software

Fig.3 shows the flow chart of digital twin software for thermal characteristics. To begin with, the operating parameters of the system should be set in the initialization interface, which include the selecting of storage address of the result file, the setting of relevant parameters and boundary conditions of the spindle and the address of batch files. Then, the macro files based on these data and the corresponding parameter macro file will be created by using Qt's QFile library. Via setting the working directory and job name in the Mechanical APDL Product Launcher, the batch execution commands can be acquired and saved in the .bat file. In Qt, use the openUrl statement in the QDesktopServices library to start the Mechanical APDL Batch program to run in the background. After the settings are completed, the IoT-DAS will be connected through the socket to establish data transmission between the spindle and the computer.

By clicking the enter button, the calculation module of the software interface is called as shown in Fig. 4, and the ANSYS Mechanical APDL Batch program is executed in the background. The batch processing controls the simulation process and result output in the form of a command stream, which makes ANSYS possess excellent separability and operability, and the thermal boundary conditions is modified in the form of a new command stream that is generating by software according to the calculation results. The data collected during the work of the spindle and the thermal characteristic data corresponding to the virtual entity are stored for later analysis.

The ANSYS simulation is solved based on the finite element method. According to the setup, it will automatically create models, divide meshes, add constraints and loads in the background as well as the process of solving and viewing the results in the light of the command stream file. Because of the use of parametric language, it can be easily modified at any step, which provides a basis for online correction of the thermal boundary conditions.

This paper uses the simulation analysis of transient thermal-structure coupling in accordance with the generated macro files file.dat opened by the .bat file. Since the calculation time depends on the difficulty of the calculation model and the computer performance, the simulation time step is selected as 80 seconds after testing. The simulation time step is set to 10 seconds. The program automatically checks the difference of the measured data and the simulated data every 80 seconds, and the thermal boundaries are corrected through the relevant mathematical model. The correction of the thermal boundary is controlled by the internal function of the programming language. The software reads the ANSYS analysis results, that is, the temperature data of each measurement point. At the same time, it finds the data corresponding to the simulation result in the actual measurement data received from the IoT-DAS, and calculate the required value and input it to the correction function. The output result of correction function is to correct the thermal boundaries, and then use the QFile to write the thermal boundaries into the parameter macro file correction parameters.mac, which will be read and updated when the next simulation cycle arrives. In this way, a correction of the boundary conditions is achieved. After correction, write the macro file through the APDL command (*use) and replace it with the corresponding part of the main command stream file. When a solution is finished, the node temperature value NodeTemp.dat file at the end of the solution will be derived as the initial condition for the thermal deformation analysis.

The solution result is output every 10 seconds, and the output visualization result can be seen through the Qt's table widget to see the actual value of the data, or through the dynamic line graph to see the temperature changing trend. When all the work is done, the experiment results are saved in the set file path.

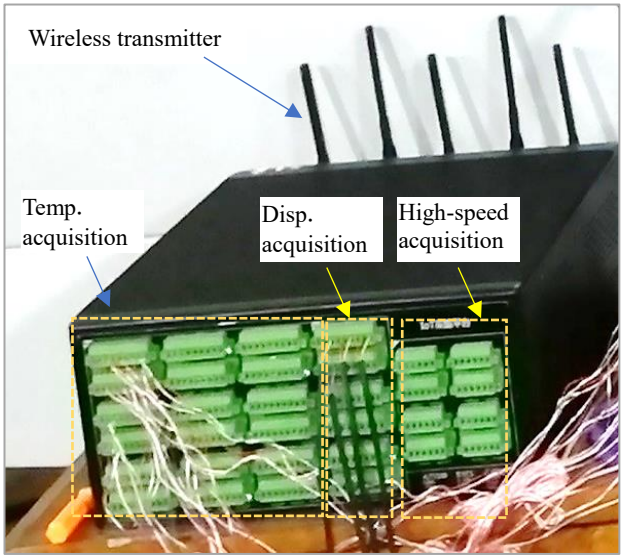

Fig. 5 IoT-based data acquisition system

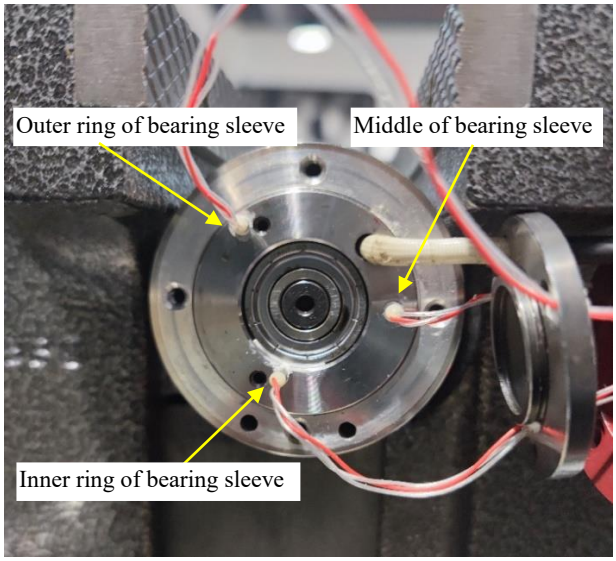

Fig. 6 The setup of temperature sensors

3.2 Design of data acquisition system

The IOT-based data acquisition device (as shown in Fig. 5) is responsible for collecting and transmitting the temperature and thermal deformation data of the physical entity measured at the thermal key points in real time. It adopts the Transmission Control Protocol/Internet Protocol (TCP/IP) to transmit data to the client, and the client creates a Socket describing the IP address and port, sending it to the server to initiate a TCP connection to the server. The server must also prepare at least two Sockets. One welcoming socket is in charge of accepting the connection request of client, that is, PC and the other is to create a corresponding connection socket to communicate with the client when receiving the client's connection, thereby establishing a TCP network connection between the collection device and the computer. After the connection is built, the data information acquired by sensors is responded to the client socket through a message, and the client parses the response message to obtain the data.

As shown in Fig. 5, the IoT-based data acquisition system include four modules which are the temperature acquisition module, the displacement acquisition module, the high-speed acquisition module which is used for high frequency data collection, and the wireless transmitter module which is used to transfer data with PC. Using the IoT-based data acquisition system can establish the mapping of thermal boundaries between the physical entities and virtual entities.

3.3 Design of physical model

There are many contact surfaces of a motorized spindle, which include the contact surfaces between the bearings and the bearing sleeves and core spindle, the contact surface between the stator and water jacket, the contact surface between the bearing sleeves and water jacket, the contact surface between the rotor and core spindle, etc. In order to obtain the actual thermal boundaries of the motorized spindle, three temperature sensors are embedded in the motorized spindle to measure the temperature of inner ring of bearing sleeve, outer ring of bearing sleeve, and middle of bearing sleeve as shown in Fig. 6.

The measured temperatures of these three points are used to correct the thermal boundaries according to the correction models. The temperature difference between the water jacket and the rear bearing sleeve is used to correct the thermal contact resistance between their contact surfaces, and the temperature difference between the rear bearing sleeve and outer ring of rear bearing is used to correct the thermal contact resistance between their contact surfaces. The heat generation of bearing is corrected as follows, calculation the difference (Δt_{mi}) between the measured temperature and initial temperature at these three points firstly, then calculation the difference (Δt_{ms}) between the measured temperature and simulated temperature at these three points, and the average ratios ($\Delta t_{ms}/\Delta t_{mi}$) at these three points are used to correct the heat generation of bearing.

It should be noted that there are some thermal boundaries that are not convenient to embed sensors such as the rotatory spindle, stator, and rotor, etc. In order to solve this problem, the surface temperatures related to the built-in motor and front bearing are used to correct the thermal boundary conditions using the correction models. Thereby, all thermal boundaries of the motorized spindle can be identified and corrected using the measured temperatures of thermal key points.

4. Correction principle of thermal boundaries

4.1 Heat generation correction

The main heat sources of a motorized spindle are the heat generated by the frictional of bearings' rotation and the heat converted by the loss of spindle motor. The loss of motor includes mechanical loss, electrical loss, and magnetic loss. The mechanical loss comes from the friction of air gap between the rotor and the stator when the rotor rotates at high speed, which is mainly related to the speed. It occurs at both ends of the rotor and the gap between the stator and the rotor, and can be calculated as,

$$P_n = \pi C \rho \omega^3 r_z^4 L$$

where, P_n is the mechanical power loss in Watts, C is the friction coefficient, ω is angular velocity in rad/s, ρ is density

of air in kg/m^3, r_z is the radius of rotor in meter, L is the length of rotor in meter.

Electric loss is the power loss that occurs when the current passes through the stator conductor coil, which is mainly related to the magnitude of the current. It occurs at the stator and is calculated by the Joule-Lenz law as,

$$P_e = \rho I^2 R$$

where, P_e is electrical power loss in Watts, ρ is conductor resistivity, I is winding current of stator in Ampere, R is conductor resistance of single-phase winding in Ω.

Magnetic loss is the loss formed by the eddy current and hysteresis of the stator and rotor cores, including eddy current loss and hysteresis loss. Eddy current loss is caused by the vortex current generated by the electromagnetic induction of the iron core under the alternating magnetic field of alternating current. Hysteresis loss is that the iron core is alternately demagnetized and magnetized under the action of a periodic magnetic field, which can be calculated as,

$$\begin{cases} P = P_w + P_h \\ P_w = \dfrac{\pi\delta^2 (f B_{\max})^2}{6\rho r_c} \\ P_h = C_h f B_{\max}^a \end{cases}$$

where, P is the eddy current power loss in Watts, δ is the thickness of rotor in meter, f is magnetic field change frequency in Hz; B_{max} is maximum magnetic induction intensity in T, ρ is iron core resistivity in Ω·m, r_c is the iron core density in kg/m^3, P_h is hysteresis power loss in Watts, C_h is the constant related to rotor material grade, a is the empirical constant, when B_{max}<1T, a=1.6, when B_{max}>1T, a=2.

When the motorized spindle rotor runs at high speed, the friction between the inner and outer rings of the bearing and the bearing rolling elements generates heat. The heat generation is mainly related to the spindle speed and total friction torque. The heat generated by bearing's rotation can be calculated by the Palmgre empirical formula,

$$Q_b = 1.047 \times 10^{-4}$$

where, Q_b is the heat generated by bearing in Watts, n is the spindle rotor speed in rpm, M is the total friction torque in N·mm.

The amount of heat generation is closely related to the total friction torque. The total friction torque is mainly composed of viscous friction torque and load friction torque. The total friction torque can be calculated as,

$$\begin{cases} M = M_n + M_z \\ M_n = 10^{-7} f_0 (vn)^{\frac{2}{3}} D_m^3, & (vn \geq 2000) \\ M_n = 160 f_0 D_m^3, & (vn < 2000) \\ M_z = f_1 P_1 D_m \end{cases}$$

where, M is the total friction torque in N·mm, M_n is the viscous friction torque related to speed in N·mm, f_0 is the coefficient related to lubrication mode, v is the lubricant kinematic viscosity in mm^2/s; D_m is the average bearing diameter in millimeter, M_z is the load friction moment in N·mm, f_1 is the factor related to bearing type and load, P_1 is the load on bearing in Newton.

For a certain bearing, the heat generation Q_b is affected by the speed n, the load P_1 and the kinematic viscosity v according to the formulas (4) and (5). Besides, the load P_1 is proportional to the temperature. On the basis of the formulas (4) and (5), through the measurement of the temperature of the thermal key points, a correction model of the heat generation of the bearing under the thermal coupling is established as,

$$\begin{cases} Q_b = 1.047 \times 10^{-4} n (M_n + M_z) \\ M_n = 10^{-7} f_0 (v(\Delta t) n)^{\frac{2}{3}} D_m^3, & (vn \geq 2000) \\ M_n = 160 f_0 D_m^3, & (vn < 2000) \\ M_z = f_1 P_1 (\Delta t) D_m \end{cases} \quad (6$$

where, $v(\Delta t)$ is the kinematic viscosity of lubricant with temperature change in mm^2/s; $P_1(\Delta t)$ is the load on bearing with temperature change in Newton.

The application of formula (6) can calculate the heat generated by the bearing at different temperatures. In order to simplify the calculation, Fan [9] proposed an empirical correction formula for bearing heat generation described as,

$$Q_b' = \frac{t_m - t_\infty}{t_f - t_\infty} Q_b \quad (3)$$

where, Q_b' is the corrected heat generation of bearing in W/m^3; t_m is the measured temperature at the thermal key points in ℃; t_f is the temperature of the motorized spindle obtained through finite element analysis in ℃; t_∞ is the environment temperature during the operation in ℃.

4.2 Thermal contact resistance correction

When stable bonding surfaces with a temperature difference transmit heat, there will be resistance between the bonding surfaces that hinders heat transmission, that is known as thermal contact thermal resistance. The rough surfaces obtained by mechanical machining are not perfectly smooth, ensuing withinside the imperfect contact between two rough surfaces. The contact occurs at finite discrete factors and the contact points display the multiscale and self-affine features. (4) The heat flux contracts at those contact points whilst the heat flux flows across joint surfaces, resulting in the difficulties of going with the drift of heat flux. The factors that affect the thermal contact resistance include pressure on the bonding surface, bonding surface material, surface roughness, gap medium, and temperature difference of the bonding surface. The contact thermal resistance R of the joint surface can be calculated by the following semi-empirical formula as,

$$\frac{r}{Rk} = 105.6 \left(\frac{P}{E}\right)^{0.68} \quad (5)$$

where, R is the initial contact thermal resistance in m^2/(K·W), r is the root mean square roughness in Micron, k is the tuned average thermal conductivity in W/(m·K), P is the pressure on the bonding surface in MPa, E is the material elastic modulus in GPa.

It can be seen from Eq. (8) that the thermal contact resistance of the joint surface of the motorized spindle is proportional to the contact pressure P. As the temperature of the spindle unit increases, the contact pressure P changes continuously. According to the radial thermal deformation formula and Hooke's law, Fan [9] proposed a correction model for the contact thermal resistance of the spindle joint

surface as,

$$R' = R\left(1 + \left(\frac{P}{EA\left(\sqrt{\frac{1+3a\Delta t}{1+a\Delta t}} - 1\right)}\right)^{0.68}\right) \tag{9}$$

where, R' is the corrected contact thermal resistance in $m^2 \cdot K/W$, A is the contact surface area in m^2, α is the thermal expansion coefficient, Δt is the temperature difference between the two adjacent temperature measurement points in ℃.

4.3 Calculation of convection coefficient

The heat generated by the stator and rotor is mainly diffused out through the water-cooling system of the spiral rectangular pipe in the cooling water jacket. The flow state of the coolant in the pipe is different, same as the heat transfer coefficient. It is necessary to judge the flow state of the cooling water according to the Reynolds number *Re*, and calculate the convective heat transfer coefficient according to the formula as,

Re<2200, laminar flow zone

$$a = \frac{\lambda}{L}\left(1.86\,\mathrm{RePr}\frac{D_H}{L}\right)^{\frac{1}{3}} \tag{10}$$

2200<*Re*<10000, the transition zone from laminar flow to turbulent flow

$$a = \frac{\lambda}{L}(0.023Re^{0.8}Pr^{0.4}) \tag{11}$$

10000<*Re*, turbulent flow zone.

$$a = \frac{\lambda}{L}\left(Re^{\frac{2}{3}} - 125\right)Pr^{\frac{1}{3}}\left(1 + \frac{D_H}{L}\right)^{\frac{2}{3}} \tag{12}$$

where, *Re* is the Reynolds constant, *Pr* is the coolant Prandtl constant, D_H is the cold zone liquid equivalent diameter in meter, λ is the coolant thermal conductivity in W/(m·K), L is the geometric characteristic length of the heat transfer surface in meter.

Using the correction models, the thermal boundaries of the motorized spindle can be corrected according to the simulated and measured temperatures. The correction models for thermal boundary conditions are written into the digital twin software for thermal characteristics to correct the thermal boundary conditions automatically.

According to the design methods abovementioned, a digital twin system for thermal characteristics can be designed to obtain the actual thermal behavior of a motorized spindle. In summary, a digital twin system for thermal characteristics includes three modules which are the digital twin software used to correct the thermal boundaries and call the ANSYS to simulate the thermal behavior of the motorized spindle, the data acquisition system used to map the thermal boundaries, and the physical entity with embedded sensors. In order to verify the effect of the proposed digital twin system for thermal characteristics, an experiment for thermal behavior of a motorized spindle is carried out in section 5.

5. Validation

5.1 Experimental setup

An experiment platform was setup for verifying the effectiveness of the proposed method based on a high-speed water-cooled motorized spindle as shown in **Fig. 7**. Three temperature sensors are embedded in the selected thermal key points of the motorized spindle as shown in **Fig. 6**, namely the outer ring of the bearing sleeve, middle of bearing sleeve, and inner ring of the bearing sleeve through drilling small holes at these thermal key points to make the PT100 temperature sensors fully fit the measuring position closely to improve the accuracy of the experiment. The punching positions are evenly distributed to reduce the impact of the error caused by the punching on the structure damage, and the holes are filled with thermally conductive silica gel to reduce the thermal contact resistance between the sensor and the measuring part. A displacement sensor is arranged at the end of the spindle to measure the axial thermal deformation of the spindle. The motorized spindle is fixed in a vise as shown in **Fig. 7**.

For data acquisition device, the function is performed by the abovementioned digital twin system for thermal characteristics, all channels are sampled once per second, and the data is processed and counted by the internal functions of the system to achieve continuous monitoring and recording of all channel information.

The material properties of the motorized spindle are listed in **Table 1**, the heat generated by the stator, the rotor, the front bearings, and the roar bearings are calculated as 5.3×10^5 W/m^2, 7.6×10^5 W/m^2, 1.45×10^6 W/m^2, and 1.04×10^6 W/m^2, respectively. There are 25 contact pairs in the spindle, and their thermal contact resistances can be calculated according to **Eq. 9**. The coefficients of nature convection and the forced convection can be calculated using **Eqs. (10, 11 and 12)**. The ambient temperature is 27℃.

Table1 Material properties of the spindle system

Parts	Material	Modulus of elasticity GPa	Poisson's ratio	Density Kg/m³	Linear expansion coefficient K^{-1}	Specific heat J/kg·K	Thermal conductivity W/(m·K)
Bearing	GCr15	219	0.3	7830	1.20×10^{-5}	460	44
Spindle	45	209	0.269	7830	1.17×10^{-5}	450	48

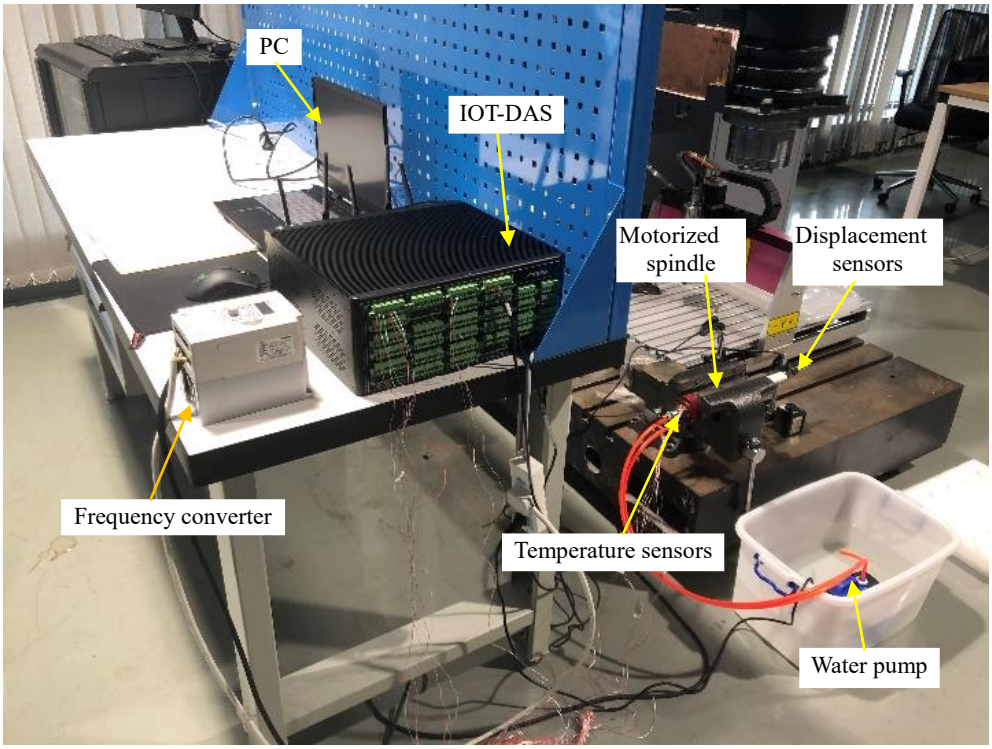

Fig.7 The experimental setup of digital twin system for thermal characteristics

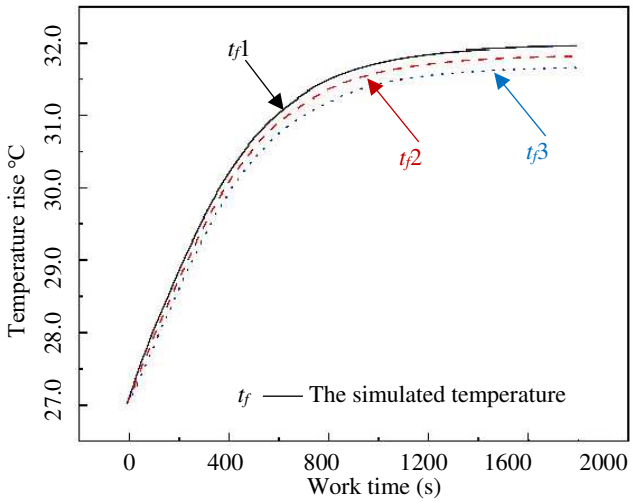

Fig.8 The temperature curve of simulation

5.2 Experimental results

In order to compare the simulation results before and after digital twin for thermal characteristics, the thermal behavior simulation of the motorized spindle before digital twin is carried out firstly. The simulation conditions are that the spindle speed is 6000 rpm, the temperatures of ambient and cooling water are all 27 ℃. The structures of the stator and bearings are simplified as cylinders, some small structures in the finite element model, such as bolts, bolt holes, chamfers, etc., are removed. Appling the calculated boundary conditions to the finite element model, the temperature rises at these three thermal key points can be obtained as shown in **Fig. 8**. It can be seen from **Fig. 8** that the thermal equilibrium time is about 1500 seconds, and the temperature rise trends of these three thermal key points are almost the same. The maximum temperature rise is 4.95 ℃ which occurs at the first thermal key point that is the inner ring of bearing sleeve. **Fig.9 (a)** shows the temperature field of the motorized spindle, the maximum temperature rise of the motorized spindle is 15.19 ℃ which occurs in the rotor. The minimum temperature rise is 2.7 ℃ which occurs in the cooling water jacket.

In order to calculate the thermal deformation of the spindle, the calculated temperature field is applied to the finite element model as a temperature load, and the displacement constraint is set to the out surface of the motorized spindle. The thermal expansion coefficients of GCr15 and 45 steel are set to 8.2×10^{-6} and 1.17×10^{-5}, respectively. **Fig.9 (b)** shows the thermal deformation of the motorized spindle, the maximum thermal deformation of the motorized spindle is 15.4 μm which occurs at the front end of the core spindle.

Next, the experiment of digital twin for thermal behavior is carried out using the digital twin system designed in section 3. The thermal contact resistance and heat generation are corrected according to the measured temperatures and the correction models established in section 4. The correction process of the thermal boundaries is carried out every 80 seconds. The experiment conditions for physical and virtual entities are that the spindle speed is 6000 rpm, the temperatures of ambient and cooling water are all 27 ℃. The initial boundary conditions are the same as the previous simulation. **Figs. (10** and **11)** show the measured and digital twin-based simulation curves of the temperature distribution at these three thermal key points and the thermal deformation of the core spindle.

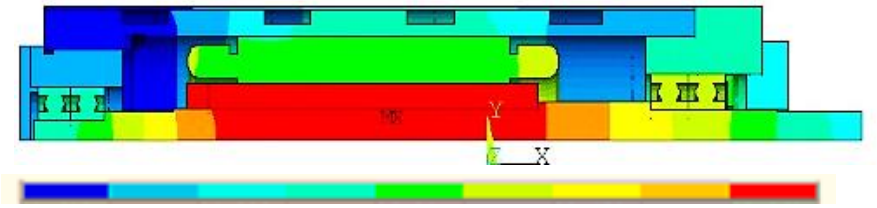

(a) Temperature field of the motorized spindle

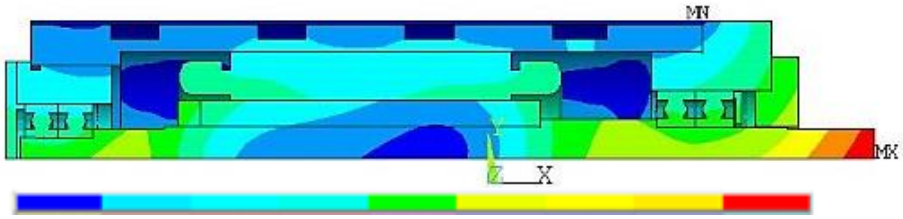

(b) Thermal deformation of the motorized spindle

Fig.9 The finite element simulation results of the motorized spindle at 1800 seconds

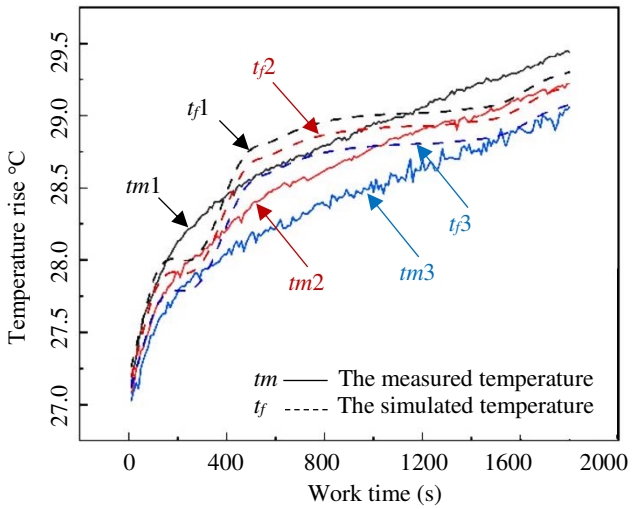

Fig.10 The measured and simulated temperature curves (tm is the measured temperature, tf is the simulated temperature)

It can be seen from **Fig. 10** that the maximum temperatures at these three thermal key points measured by the sensors are 29.06, 29.22, and 29.44 ℃, respectively, the maximum temperatures calculated by the digital twin system are 29.07, 29.20, and 29.29 ℃, respectively. The maximum error between the digital twin-based simulation results and the measured results is less than 0.36 ℃, and the calculation accuracy is greater than 98% in the whole process.

Comparing **Fig.10** with **Fig.8**, the maximum simulated temperatures at these three thermal key points before digital twin are obviously larger than that using the digital twin system. The maximum temperature rise using the digital twin system is reduced 2.66 ℃ compared traditional simulation. That is, the simulation effect of the proposed digital twin system is significantly better than traditional simulation. That is, the calculated thermal boundary conditions are difficult to be close to the true value due to the influence of many factors. The simulation results also show that the simulated temperature curves at these three thermal key points before digital twin are inconsistent with the measured temperature curves. The simulated thermal equilibrium time before digital twin is about 1500 seconds, however, the measured temperatures are always rising, this is because the continues change of thermal contact resistance caused by the thermal deformation. Therefore, the digital twin for thermal behavior is of great significance to improve the accuracy of thermal characteristics simulation.

Fig.10 also shows that the temperature curves simulate by the digital twin system gradually converge to the measured temperature curves. That is, the correction of the thermal boundaries is a process of gradual convergence. In order to reduce or eliminate the oscillation in the convergence process, the correction models for thermal boundaries or correction method should be improved.

The thermal deformation of the front end of the motorized spindle simulated by the digital twin system is output every 80 seconds. And the measured thermal deformation at the same time is processed by calculating the average value. **Fig.11** shows the measured and simulated thermal deformation curves, the accuracy of the prediction result can reach about 95%. Therefore, the proposed digital twin for thermal behavior can effectively improve the simulation accuracy of thermal characteristics of the motorized spindle, it has a guiding role in improving the thermal optimization design of high-speed motorized spindle.

6. Conclusions

A digital twin system for thermal characteristics is proposed based on the mapping and correcting of thermal boundary conditions. The proposed digital twin system includes three modules which are the digital twin software, the data acquisition system, and the physical model with embedding sensors. The experimental results show that the prediction accuracy of the digital twin system is greater than 95%. According to the simulation and experiment results, the following conclusions can be drawn.

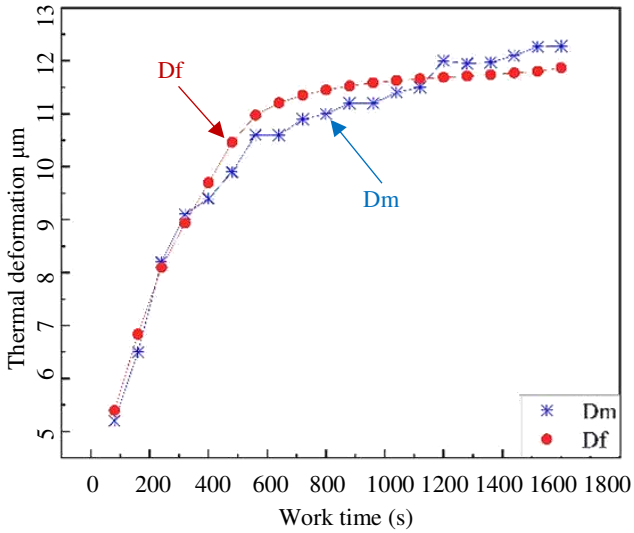

Fig.11 Thermal deformation of the core spindle (Dm is the measured displacement, Df is the calculated displacement)

(1) The simulated and measured temperature rises at thermal key points can be used to correct the thermal boundary conditions using the correction models which can be established according to the empirical formulas.
(2) The digital twin system can be designed through mapping the thermal boundaries of physical entity to the virtual entity to simulate the thermal characteristics of a motorized spindle using the embedded sensors and secondary development of ANSYS.
(3) Experimental results show that the prediction accuracy of temperature field can reach 98%, and the prediction accuracy of thermal deformation can reach 95%.

The high-precision prediction results show that the digital twin technology has great potential in the field of thermal characteristics research, which is of great significance for improving the accuracy of thermal characteristics simulation and thermal optimization.

Funding information This paper is sponsored by the "Technology of on-line monitoring system for thermal characteristics of NC machine tools" (No. H2019304021); the "Project funded of Shanghai science committee- Precision technology and its application for five-axis machine tool based on the real-time compensation" (NO. J16022).

Compliance with ethical standards

Conflict of interest The authors declare that they have no conflict of interest.

Data availability The data that supports the findings of this study is available from the corresponding author upon reasonable request.

Reference

1. GRIEVES M (2016) Digital twin: manufacturing excellence through virtual factory replication [EB].
2. Kostenko D, Kudryashov N, Maystrishin M, et al (2018) Digital twin applications: diagnostics, optimization and prediction[J]. Annals of DAAAM & Proceedings
3. Tao F, Cheng J, Qi Q, Zhang M, Zhang H, Sui F (2018) Digital twin driven product design, manufacturing and service with big data. Int J Adv Manuf Technol 94:3563–3576
4. Tao F, Sui FY, Liu A et al (2018) Digital twin-driven product design framework. Int J Prod Res 57(12):3935–3953
5. Tao F, Zhang M, Liu Y, Nee AYC (2018) Digital twin driven prognostics and health management for complex equipment. CIRP Ann 67(1):169–172
6. Lu Y, Liu C, Wang K, Huang H, Xu X (2020) Digital twin-driven smart manufacturing: connotation, reference model, applications and research issues. Robot Comput Integr Manuf 61:101837.
7. Schleich B, Anwer N, Mathieu L, Wartzack S (2017) Shaping the digital twin for design and production engineering. CIRP Ann Manuf Technol 66(1):141–144
8. Wei YL, Hu TL, Zhou TT, Ye YX, Luo WC (2020) Consistency retention method for CNC machine tool digital twin model. J Manuf Syst.
9. Liu XJ, Ni ZH, Liu JF, Cheng YL (2016) Assembly process modeling mechanism based on the product hierarchy. Int J Adv Manuf Technol 82(1-4):391–405
10. Zidek K, Pitel J, Adamek M, Hosovsky A (2020) Digital twin of experimental smart manufacturing assembly system for industry 4.0 concept. Sustainability 12(9):3658
11. Qi Q, Tao F (2018) Digital twin and big data towards smart manufacturing and industry 4.0: 360 degree comparison. IEEE Access 6:3585–3593
12. Qi Q, Tao F, Zuo Y, Zhao D (2018) Digital twin service towards smart manufacturing. Procedia CIRP 72:237–242
13. ZHENG Y, YANG S, CHENG H (2019) An application framework of digital twin and its case study [J]. Journal of Ambient Intelligence and Humanized Computing 10(3):1141-53
14. W. Luo, T. Hu, W. Zhu, F. Tao (2018) Digital twin modeling method for CNC machine tool[C], 2018 IEEE 15th International Conference on Networking, Sensing and Control (ICNSC), 2018:1-4
15. Eric J. Tuegel, Anthony R. Ingraffea, Thomas G, et al (2011) Eason reengineering aircraft structural life prediction using a digital twin[J]. International Journal of Aerospace Engineering 8(2):1-14
16. Chen DJ, Bonis M, Zhang FH, Dong S (2010) Thermal error of a hydrostatic spindle. Precis Eng 35:512–520
17. Su H, Lu LH, Liang YC, Zhang Q, Sun YZ (2014) Thermal analysis of the hydrostatic spindle system by finite volume element method. Int J Adv Manuf Technol 71:1949–1959
18. Zhou H, Fan K, Gao R (2020) Fast heat conduction-based thermal error control technique for spindle system of machine tools[J]. The International Journal of Advanced Manufacturing Technology 107(1): 653-666.
19. Xu M, Jiang S (2011) A thermal model of a ball screw feed drive system for a machine tool [J]. Proceedings of the Institution of Mechanical Engineers, Part C: Journal of Mechanical Engineering Science 225(C1):186–193
20. Jian L, Kim DH, Lee CM (2015) A study on the thermal characteristics and experiments of high-speed spindle for machine tools. Int J Precis Eng Manuf 16:293–299
21. Fan K (2017). Research on the machine tool's temperature spectrum and its application in a gear form grinding machine[J]. The International Journal of Advanced Manufacturing Technology 90(9): 3841-3850.
22. Zhang L, Xuan J, Shi T, et al (2020) Robust, fractal theory, and FEM-based temperature field analysis for machine tool spindle[J]. The International Journal of Advanced Manufacturing Technology 111(5): 1571-1586.
23. Liu J, Ma C, Wang S, et al (2019) Thermal contact resistance between bearing inner ring and shaft journal[J]. International Journal of Thermal Sciences 138: 521-535.
24. Liu T, Gao WG, Zhang DW, Zhang YF, Chang WF, Liang CM, Tian YL (2017) Analytical modeling for thermal errors of motorized spindle unit. Int J Mach Tools Manuf 112(1):53–70
25. Huang JH, Than VT, Ngo TT, Wang CC (2016) An inverse

method for estimating heat sources in a high speed spindle. Appl Therm Eng 105:65–76
26. Chow JH, Zhong ZW, Lin W, Khoo LP (2012) A study of thermal deformation in the carriage of a permanent magnet direct drive linear motor stage. Appl Therm Eng 48(12):89–96